Mechanical Properties and Histological Evaluation of Bone Grafting Materials Containing Different Ratios of Calcium Phosphate Cement and Porous β-tricalcium Phosphate Granules

Hirokazu TANAKA[1)2)], Shin-ichi YAMADA[1)*], Hitoshi AIZAWA[1)]
Kiyonori HAYASHI[1)], Tetsu SHIMANE[1)], Imahito KARASAWA[1)]
Nobuhiko YOSHIMURA[1)], Fumihiro NISHIMAKI[1)], Yuko ARAKAWA[1)] and Hiroshi KURITA[1)]

1) *Department of Dentistry and Oral Surgery, Shinshu University School of Medicine*
2) *Department of Dentistry and Oral Surgery, Aizawa Hospital*

Objective : Although calcium phosphate cement (CPC) is a bone substitute material having good formativeness, biocompatibility, and osteoconductivity, it has very slow biodegradability in vivo. This study aimed to create a new porous bone cement with enough strength, good formativeness, biodegradation, and osteoconductivity for bone regeneration by adding porous β-tricalcium phosphate (β-TCP) granules to CPC.

Methods : A commercially available CPC and porous β-TCP were used in this study. Three testing materials with different mixing ratios of CPC and β-TCP (C0, C30 and C50, having mixing ratios of β-TCP of 0, 30, and 50 wt%, respectively) were examined. We evaluated the basic materialological properties in vitro. In addition, biodegradation and osteoconductivity were evaluated in vivo by implantation in rabbit femurs.

Results : The setting times for C30 (15 minutes) and C50 (18 minutes) were thought to be within a clinically acceptable range. Although the compressive strength decreased with increasing content of β-TCP, that of C50 was the same as for cancellous bone. The porosity and permeability increased with addition of more β-TCP granules. Histological evaluation revealed that biodegradability of the material increased with the addition of more β-TCP granules and the material had good bioactivity. Notably, at 36 weeks after implantation, C50 was almost completely resorbed and replaced by regenerated bone.

Conclusions : The results of this study suggested that the composite created by adding equal weight percent of porous β-TCP granules to CPC paste had good biodegradability and adequate mechanical strength, and was adaptable as a bone substitute for bone defect repairs. *Shinshu Med J 66 : 139—150, 2018*

(Received for publication November 22, 2017 ; accepted in revised form December 28, 2017)

Key words : calcium phosphate cement, β-TCP, bone regeneration, bone replacement

I Introduction

Various calcium phosphate cements (CPC) have been studied for application as bone substitutes[1)-10)]. CPC paste has been used in bone reconstruction because of its ability to be shaped similarly to the bone defect. Although CPC has been reported to have excellent biocompatibility and osteoconductivity[10)-12)], its very slow biodegradability must be improved to promote bone regeneration. As the reaction of CPC progresses, hydroxyapatite (HA) is precipitated[13)]. HA is hardly absorbed in vivo. Especially in oral and maxillofacial surgery, non- or slow biodegrading bone materials might carry a higher risk of infection. One way to improve bioabsorption and bone replacement is to increase the porosity of hardened CPC.

β-tricalcium phosphate (β-TCP) has been widely used as a bone substitutional material for bone re-

* Corresponding author : Shin-ichi Yamada
Department of Dentistry and Oral Surgery,
Shinshu University School of Medicine,
3-1-1 Asahi, Matsumoto, Nagano 390-8621, Japan
E-mail : yshinshin@shinshu-u.ac.jp

generation because of its excellent biocompatibility[14)15)]. β-TCP biodegrades more rapidly than crystalline HA[16)-19)]. Porous β-TCP is considered to be a more suitable scaffold for bone formation than HA[20)]. However, β-TCP has some problems such as poor mechanical strength and formativeness.

By taking advantage of the formability and strength of CPC and the bioabsorbability and osteoconductivity of β-TCP, we tried to create new porous bone cement composed of porous β-TCP granules and CPC with sufficient strength, good formativeness, and biodegradation for bone regeneration. We mixed porous β-TCP and CPC paste to create a composite containing macro- and micropores. Its mechanical properties, micro- and macro-structures were examined in vitro, and biodegradation, biocompatibility, and osteogenesis in vivo.

Ⅱ Materials and Methods

A CPC and β-TCP

The CPC used in this study was Cerapaste® (NGK Spark Plug Co. Ltd, Aichi, Japan). It consists of mixed powder and liquid. The powder contains tetracalcium phosphate (TeCP : 67.5wt%) and dibasic calcium phosphate anhydrous (DCPA : 32.5%), and the liquid contains water and dextran sulfate sodium. The hardening reaction of the CPC is temperature dependent ; it starts hardening promptly at 37 ℃ (near body temperature), and hardens slowly at 25 ℃ (near room temperature), and finally hardens as HA.

The β-TCP used in this study was Cerabeta® granules (NGK Spark Plug Co. Ltd, Aichi, Japan) with a diameter of 0.6-1.0 mm. The granule has a hollow interior and porous shell. The porosity of Cerabeta® granules is 35%, the macroporosity is 200 μm, and the microporosity is one μm in diameter. CPC and β-TCP were kindly provided by NGK Spark Plug Co. Ltd.

B Fabrication of study samples (composite of CPC and β-TCP granules with different ratios)

Three testing samples with different mixing ratios of β-TCP granules to CPC (C0, C30, and C50, having mixing ratios of β-TCP of 0, 30, and 50 wt%, respectively) were prepared. At first, the CPC powder was kneaded with the malaxation liquid for 60 seconds. Thereafter, different wt % of β-TCP granules was added into the CPC paste and was softly mixed for 30 seconds at room temperature. The CPC powder/malaxation liquid (P/L) ratio was 3.57 for C0, 3.18 for C30, and 2.1 for C50 in order to achieve the same final consistency.

In vitro study

C Consistency

The consistency of the composite paste was measured using the following procedures : one gram of the paste-like samples just after kneading was gently placed on a glass plate, then another 120 g glass plate was gently placed on the paste and the longest and shortest diameters of the spread paste were measured in mm. The measurements were carried out five times and the values averaged.

D Measurement of paste setting time

The mixed composite cement paste was placed in a ring (internal diameter : 10 mm, width : 7 mm) and flattened on its top surface. The paste was then incubated at 37 ± 1 ℃ and 95% to 100% humidity. A flat-tipped 2-mm-diameter needle was gently placed on the top surface at different time points. The setting time was defined as the time at which no indent was formed by the needle (300 g in weight). Measurement was carried out 5 times and the values averaged.

E Measurement of the compressive strength of the hardened body

The mixed composite cement paste was injected into plastic cylindrical containers (internal diameter : 7 mm ; height : 14 mm). After setting, the hardened body was immediately picked-up and immersed in distilled water (DW) and incubated at 37 ± 1 ℃ for one day, and then used for measurement of compressive strength. Compressive strength was measured using a universal testing machine (AG-100kNISMO®, Shimadzu Corporation, Kyoto, Japan) with a crosshead speed of 0.5 mm/min, and the mean value of 5 samples was calculated.

F Density and Porosity

To estimate the bulk density and total porosity of the hardened body, samples were prepared in the same way as for measurement of compressive strength. The total porosity (P) of the specimens was calculated as follows : dry weight (M) of each specimen was divided by volume (V) to obtain density (D). This was divided by the theoretical density of hydroxyapatite (DHAp = 3.16 g/cm^3), subtracted from 1, and expressed as a percentage.

D = M/V (1)

P = 100 × (1−D/DHAp) (2)

D = Density

M = Dry Weight

V = Volume

P = Porosity

DHAp = Density of hydroxyapatite = 3.16 g/cm^3

G SEM micrographs of the cross-section of the hardened-body

The surface morphology of the gold coated hardened body was analyzed by scanning electron microscopy (SEM, Stereoscan S360 Cambridge Ltd.) at an operating voltage of 20 kV and electrical current of 10 mA.

H X-ray computed microtomography of the hardened body

After one day soaking in DW, the hardened body was scanned using 3D micro-CT (CosmoScan, Rigaku Corp., Tokyo, Japan). The X-ray source operates at 90 kV and 150 μA, scan time 8 min, image range (9.6 × 9.6 mm) and voxel size (20 × 20 × 20 μm). I-view-R (J. Morita Mfg. Corp., Kyoto, Japan) was used as the viewer.

I X-ray diffraction analysis (XRD)

The phase composition of each synthesized material after 2 days soaking in DW was checked by XRD (Ultima IV, Rigaku Corp., Tokyo, Japan) with Cu-kα radiation operated at 40 kV and 40 mA in continuous scanning mode at a step size of 0.02° and a scanning rate of 2.00°/min.

J Penetration test

Each hardened-body (cylinder-shaped ; 7 mm in diameter and 14 mm in height) was immersed in a red-colored propylene glycol solution for 24 hours. Thereafter, a horizontal section at the representative center height was cut using a model trimmer (Y-230, Yoshida Dental Distribution Co. Ltd., Tokyo, Japan), and the red-stained area was measured using NIH ImageJ software (National Institutes of Health, Bethesda, MD). The average of 5 samples was calculated. The penetration rate (Pr) was calculated according to the following formula :

Pr = red stained area / total area × 100%

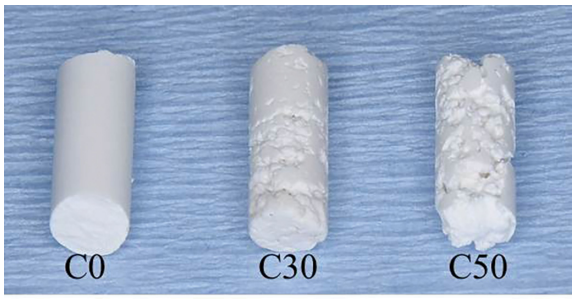

Fig. 1 Implants (hardened composites) with different CPC/β-TCP ratios
The surface is rough as the mixing ratio of β-TCP increases.

In vivo study

K Implantation of the samples

Six male New Zealand white rabbits weighing between 3.5 and 4.0 kg were used for this study. All of the surgical procedures were performed under general and local anesthesia by administering 3% pentobarbital (30 mg/kg/i.v. Somnopentyl ; Kyoritsu Seiyaku, Japan) and 2% lidocaine (1 ml i.m. ; AstraZeneca, Osaka, Japan). A cylindrical defect through the cortical bone surface into the cancellous bone was prepared with a trephine drill (4 mm diameter and 10 mm depth) in the lateral epicondyle of the bilateral femora at a low rotational speed under continuous saline cooling. Subsequently, each defect was filled with already-hardened implant materials and then closed with sutures in layers. Each implant material was made by filling a cylinder (cylinder-shaped ; 4 mm in diameter and 10 mm in height) and incubating at 37 ± 1 ℃ and 95% to 100% humidity for 30 min **(Fig. 1)**. The left and right femora were randomly assigned to receive study samples (C0, C30, and C50). The samples were placed in 12 femur bones of 6 rabbits. Postoperatively, penicillin was admin-

istered to prevent infection (50000 IU/kg) for 3 days. The animal protocol was approved by the Committee for Animal Experiments of Shinshu University (Approval Number #280022).

L Histological evaluation

After 4, 12 and 36 weeks, rabbits were sacrificed by an overdose of pentobarbital. All samples including surrounding bone tissue were extirpated en bloc, fixed by immersion in 10% neutral buffered formalin, and subjected to histological assessments. For histomorphometric examination, the thigh bone samples were dehydrated in a graded series of ethanol, embedded in light-curing resin (Technovit 7200 VLC, Kulzer, Wehrheim, Germany), and cut into sections 150 μm in thickness with a diamond saw (Cutting Grinding System, BS-300CP band system, EXAKT, Apparatebau, KG, Norderstedt, Germany). Sections were then ground to a thickness of about 60 μm with a micro-grinding system (400 CS micro grinding system, EXAKT Norderstedt, Germany). The section used for staining was cut at the center of the sample. These bone samples were stained with 5% toluidine blue, and examined with a light microscope (Biorevo BZ-9000, Keyence, Osaka, Japan).

Biodegradation of the implant material (absorption rate) was measured using NIH ImageJ software (National Institutes of Health, Bethesda, MD). Regions of interest (ROI ; 1.5 mm in length and 1.5 mm in width) were set randomly in 3 central and 3 surface areas in each histological section (toluidine blue staining). The absorption rate (Ar) was calculated using the following formula : Ar = area of ROI − area of residual sample / area of ROI × 100%

M Statistical analysis

Statistical analysis was performed using one-way ANOVA, Kruskal Wallis test and Wilcoxon test by means of SPSS 13.0 computer software (SPSS Inc, Chicago, IL, USA). P values less than 0.05 were considered significant.

Ⅲ Results

In vitro study

A Setting time

The malaxation conditions (liquid-to-powder ratios, L/P ratio), consistency, and setting times for the composite pastes with different mixing ratios of β-TCP granules to CPC are shown in **Table 1**. Using the recommended malaxation conditions (L/P ratio : 3.57), the setting time of CPC cement was 10 ± 1.09 minutes. To get the same consistency as the CPC cement, C30 and C50 required L/P ratios of 3.18 and 2.10, respectively. The setting time increased with additional β-TCP to 15 ± 1.72 minutes for C30 and 18 ± 1.41 for C50. The setting time of the composite had a direct relation with the mixing ratio of β-TCP.

B Compressive strength

Fig. 2A shows the compressive strengths of C0, C30, and C50. There was a significant difference among them (Kuruskal-Wallis, $p<0.05$). The compressive strength of C0 was 28 MPa (median). As β-TCP content increased, the compressive strength significantly decreased ; the median of compressive strength of C30 was 22 MPa and that of C50 was 13 MPa.

C Total porosity rate

The total porosity rates of the hardened composites are shown in **Fig. 2B**. There was a significant difference among the different mixing ratios of β-TCP granules to CPC (Kruskal Wallis test, $p<0.05$). Porosity rates increased with increasing β-TCP content (median ; 27% in C0, 31% in C30, and 36% in C50).

D SEM micrograph

The surface morphology of the cross-section of hardened composite was observed by SEM **(Fig. 3)**. C30 and C50 were increasingly rough on the surface in that order. In addition to the macropores of β-TCP granules, CPC cement had other macropores or fissures. In C30 and C50, CPC cement was present between the β-TCP granules and adhered to them. The macropores of the β-TCP granules were present without any involvement of CPC cement in both C30 and C50.

E Micro-Computed Tomography (Micro-CT)

Several shapes and sizes of pores were observed in the hardened composite cements **(Fig. 4)**. In C0, several sizes of macropores were observed in the CPC cement. In C30, β-TCP granules were scat-

Table 1 Setting times of composite pastes of CPC and β-TCP

	β-TCP mass%in CPC		
	CO	C30	C50
Powder/liquid ratio	3.57	3.18	2.10
Setting time (min)	10 ± 1.09	15 ± 1.72	18 ± 1.41
Consistency (mm)	20	20	20

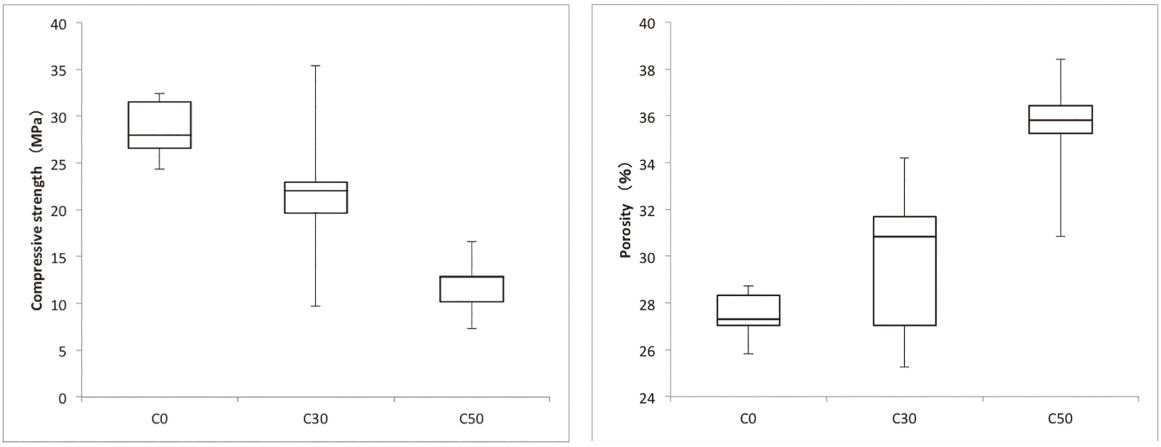

A B

Fig. 2
A : Compressive strength of hardened composites of CPC cement and β-TCP granules (n = 5).
As β-TCP content increased, the compressive strength decreased.
There was a significant correlation between compressive strength and β-TCP contents (Kruskal-Wallis test : p = 0.014).
B : Total porosity of hardened composites of CPC cement and β-TCP granules (n = 5).
Porosity of the cements had a tendency to increase with the increment of β-TCP content
There was a significant relationship between the porosity and β-TCP contents (Kruskal-Wallis test : p = 0.016).

tered among CPC cement, and macropores were mainly observed in the β-TCP granules. In C50, β-TCP granules were in contact with each other in CPC cement. Macropores were observed in both CPC and β-TCP granules. Macropores tended to increase with increasing β-TCP content. The macropores of the β-TCP granules were maintained without any involvement of CPC cement.

F X-ray diffraction (XRD) analysis

The XRD patterns of C0, C30, and C50 are shown in **Fig. 5**. The crystalline phase of CPC cement (C0) contained hydroxyapatite (HA) and tetracalcium phosphate (TeCP), resulting from the low crystallinity of CPC cement. The crystalline phases of C30 and C50 contained β-TCP, and they had decreasing amounts of HA and TeCP with increasing weight % of β-TCP.

G Penetration test

To examine the penetration rate, cross sections of hardened composites were observed after 24 hours' immersion in red solution **(Fig. 6A)**. The area stained with red solution became larger with increasing weight % of β-TCP granules. In C0, only the outer layer was stained. In C30, red solution penetrated up to 2 mm but did not reach the center part. In C50, red solution reached the center of the composite cement. Almost all of C50 was dyed with red, and its outer surface collapsed and became rough. The calculated median penetration rates were 20.5% in C0, 73.3% in C30, and 96.5% in C50. The difference was statistically significant (**Fig. 6B**, Kruskal Wallis test, $p<0.05$).

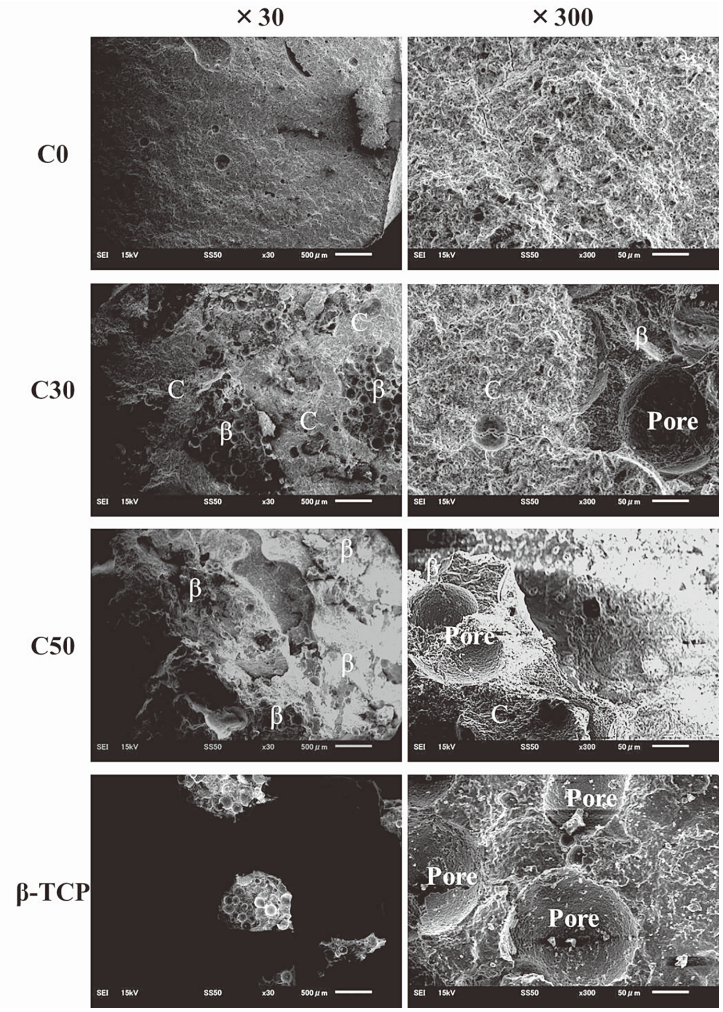

Fig. 3 Cross-section analysis of the hardened composite bodies of CPC cement and β-TCP granules
β-TCP granules were observed diffusely in C30 and C50. β ; β-TCP, ; Pore ; Macropore of β-TCP, C ; CPC.

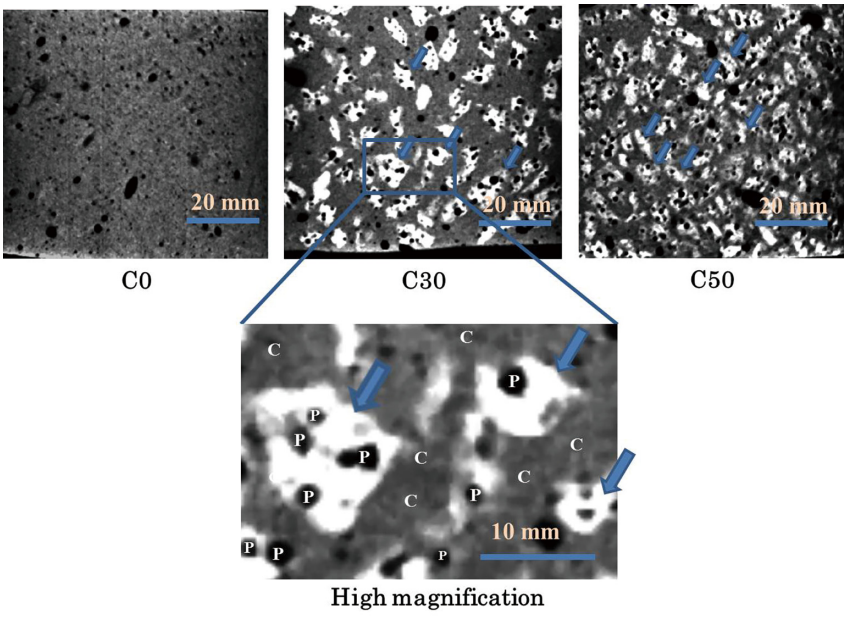

Fig. 4 Micro-computed tomography of the materials used in this study
C30 and C50 contain β-TCP granules (blue arrows). Blue arrows ; β-TCP, ; P ; Macropore of β-TCP, C ; CPC.

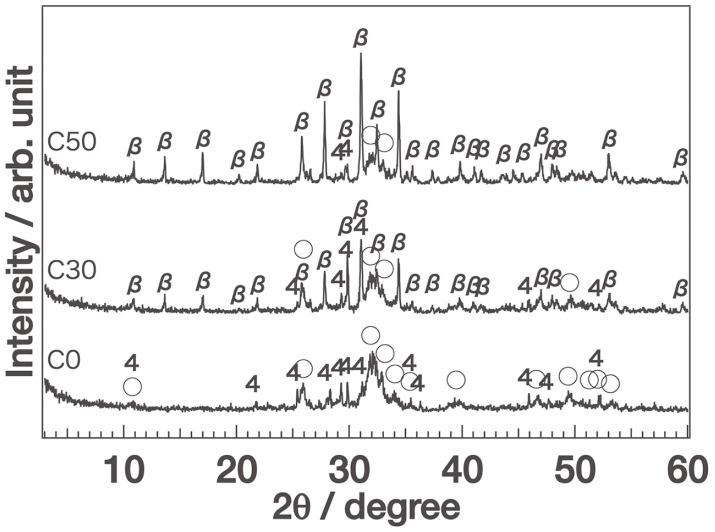

Fig. 5 X-ray diffraction patterns of cements composed of CPC and β-TCP.
As the mixing rate of β-TCP increased, the HA formations were decreased.
○ ; HA, β ; β-TCP, 4 ; TeCP.

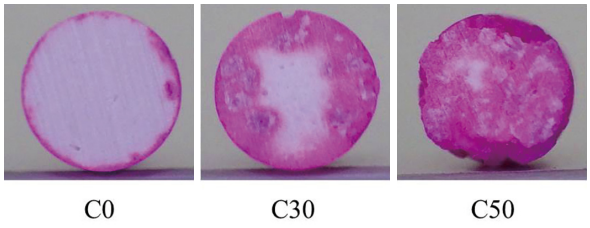

A

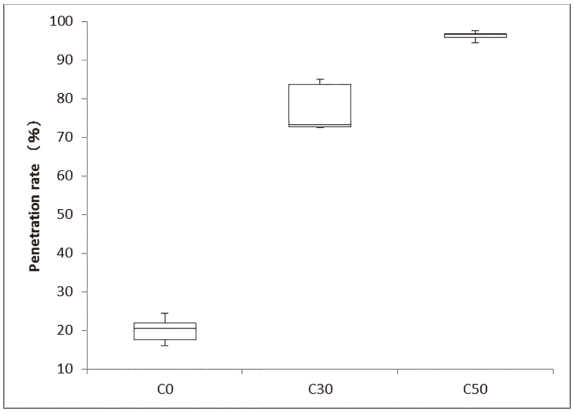

B

Fig. 6
A : Cut surfaces of cements composed of CPC and β-TCP in penetration test.
B : Penetration rates of cements composed of CPC and β-TCP (n = 5).
As the mixing rate of β-TCP increased, the penetration rate also increased.
There was a significant difference in penetration rates among C0, C30, and C50 (Kruskal-Wallis test, p = 0.002).

In vivo study

H Histological evaluation

Histological photos of each specimen are shown in **Fig. 7A**. In all samples, at 4 weeks after implantation, living bone was directly in contact with outer and inner surfaces (especially in C30 and C50) of the implanted material without any interposing tissue. The β-TCP was absorbed with time. In both C50 and C30, absorption occurred from the exposed surface of β-TCP (**Fig. 7A** : C30-12W-H, C50-12W-H). Furthermore, in C50, absorption also occurred from the inside of the implant material (**Fig. 7A** : C50-12W-L).

In C0, the living bone and the implant were closely adherented at 4 weeks after implantation. In addition, the surface of the implant material was covered with new bone (**Fig. 7A** : C0-4W-H). However, even at 36 weeks, CPC absorption was negligible.

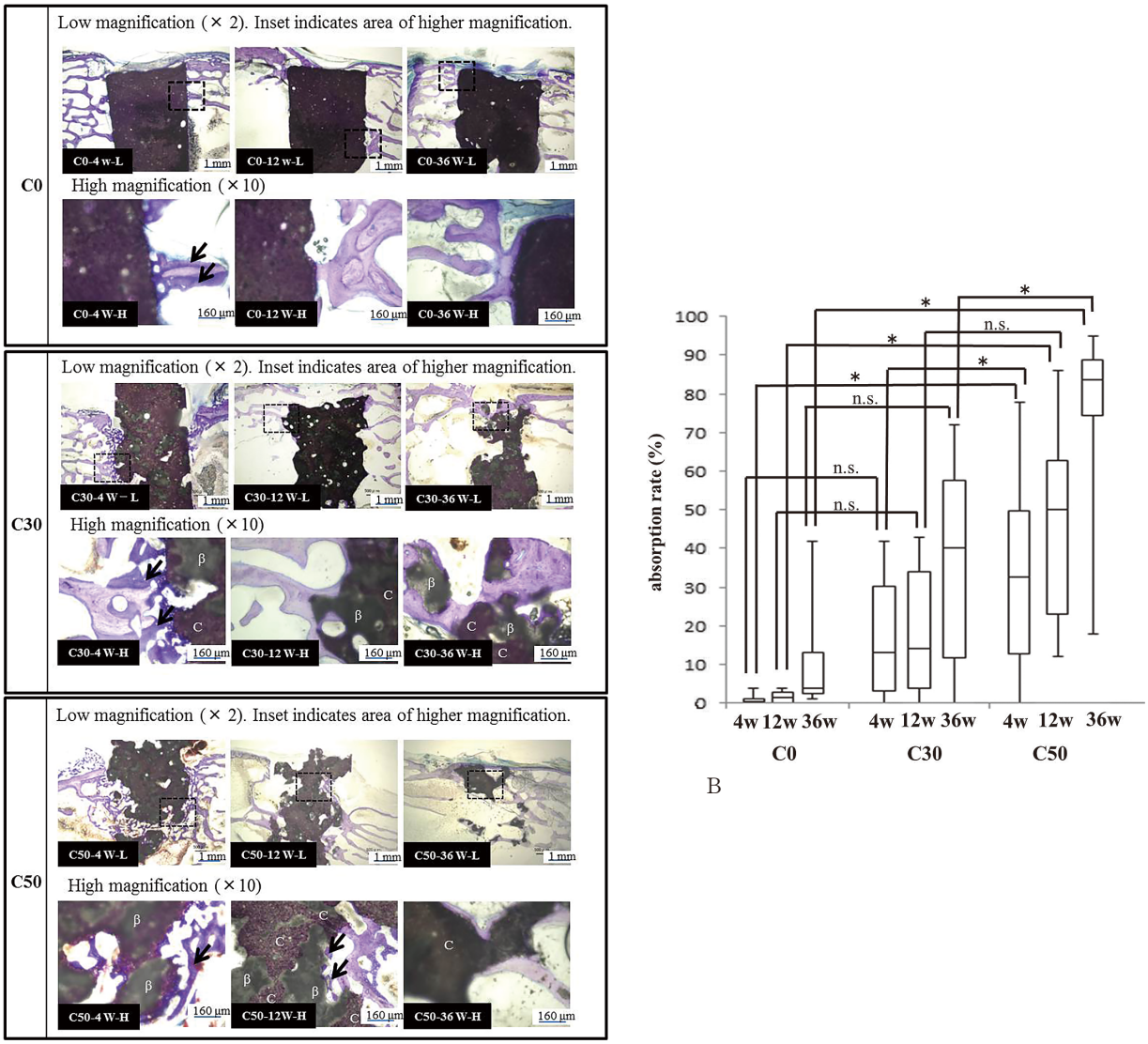

A

B

Fig. 7

A : Histological images of specimens of different composites of CPC and β-TCP cement (C0, C30, and C50) at 4, 12, and 36 weeks (H : ×10 magnification, L : ×2 magnification, toluidine blue staining).

Black arrow ; new bone area, β ; β-TCP, C ; CPC.

In C0, the living bone and the implant were closely adherented at 4 weeks after implantation. The surface of the implant material was covered with new bone. CPC absorption was negligible at 36 weeks. In C30 and C50, new bone was formed at the surface of the implant material and bone penetrated into it at 4 weeks after implantation. Bone formation could be confirmed in the interior (macropore or fistula) of the implant material (C50-4W-H). After 12 weeks, new bone was formed at the sites where β-TCP was absorbed (C50-12W-H). After 36 weeks, in C50, almost all of the implant material was absorbed, and new bone covered the remainder (C50-36W-H).

B : Biodegradation of implant material (absorption rate)

C30 showed no statistically significant difference in any period compared to C0, while C50 had a statistically significant difference from C0 in all periods (Wilcoxon test, $p<0.05$).

＊ ; $P<0.05$, n.s. ; not significant

Moreover, bone covered the entire surface of C0, but there was little penetration into the implant material (**Fig. 7A** : C0-36W-H). In contrast, in C30 and C50, new bone was formed at the surface of the implant material and bone penetrated into it at 4 weeks after implantation (**Fig. 7A** : C30-4W-L, C50-4W-L). Moreover, bone formation could be confirmed in the interior (macropore or fistula) of the implant material (**Fig. 7A** : C50-4W-H). After 12 weeks, new bone was formed at the sites where β-TCP was absorbed

(**Fig. 7A**: C50-12W-H). After 36 weeks, in C50, almost all of the implant material was absorbed, and new bone covered the remainder.

I Biodegradation of implant material (absorption rate)

In the C50 sample, 83% of material was absorbed after 36 weeks. In C0, little absorption had occurred even after 36 weeks. As the amount of β-TCP increased, the material was absorbed more quickly in vivo. C30 showed no statistically significant difference in any period compared to C0, while C50 had a statistically significant difference from C0 in all periods (Wilcoxon test, $p<0.05$).

Ⅳ Discussion

In oral and maxillofacial diseases, bone defects sometimes occur due to tumors, trauma, bone cysts, etc. Bone resorption caused by periodontal disease often results in tooth loss. β-TCP has been used widely as a bone substitute for such bone defects, because it shows good biodegradation and osteoconductivity. However, β-TCP has disadvantages such as low mechanical properties and difficulty of formativeness. CPC has been widely used clinically as a bone filler material. However, CPC has disadvantages such as poor bioabsorption and bone replacement[21]. Both materials offer a trade-off between mechanical and biological performance. Therefore, in this study, composite pastes with different ratios of CPC and porous β-TCP granules were examined to develop a new composite bone cement with adequate strength, formativeness, and good bioactivity (biodegradation, biocompatibility and osteogenesis).

Porosity and interconnectivity are important properties for bone substitute materials. Interconnecting pores are advantageous for the resorption of bone substitute and bone formation because they allow migration and proliferation of bone cells as well as vascularization. CPC is intrinsically nonporous and does not contain an interconnected network of micropores[22]. The average pore size of CPC is large enough to allow the transport of nutrients but too small to allow the entry of osteoclasts and osteoblasts to resorb the CPC and form new bone[23]. Therefore, in this study, porous β-TCP granules having macro- (200 μm) and micropores (1 μm) were mixed to create an interconnected network of macropores in the new bone composite substitute. Our results showed that the total porosity of the hardened composite increased with an increasing mix ratio of β-TCP granules to CPC. The penetration test demonstrated higher permeability with a greater percentage of β-TCP granules. Especially in C50, the red solution reached into the center of the material. These results suggested that the porosity and permeability were increased by adding more β-TCP granules. However, the type of porosity and size of pores are a key for bone substitution because high porosity and large pores enhance biodegradation and bone ingrowth into the bone substitute[24]. Micro-CT and SEM images of C50 showed that β-TCP granules were in contact with each other and the macropores of the β-TCP were not filled with CPC cement. The CPC cement did not invade the macropores of the β-TCP granules, probably because the β-TCP granules were added after the CPC cement was kneaded. These results do not definitively prove the existence of interconnecting macropores. However, there might be a possibility that the adjoining β-TCP granules and several sizes and shapes of macropores created in the CPC cement produced an interconnection of macropores. If the CPC cement invaded the macropores of the β-TCP and blocked the macropores, it was predicted that the absorption rate in vivo would obviously decrease. However, this study proved that even when CPC cement and β-TCP granules were mixed, CPC cement did not invade the pores of β-TCP granules. Therefore, as shown in the in vivo study, almost all of C50 (83%) was resorbed and replaced at 36 weeks after the implantation, compared with little resorption and replacement in C0 and C30. In the histological examination, in both C30 and C50, absorption occurred from the exposed surface of β-TCP. Furthermore, in C50, absorption also occurred from the inside of the sample. In C50, β-TCP granules existed in contact with each other. Thus, if β-TCP is absorbed, further communication of macropores (holes

where the β-TCP granules come out) would be created inside the CPC cement, which would further allow resorption of the CPC cement and migration of osteoblasts and mesenchymal cells. From these results it was suggested that C50 had sufficient porosity and a possibility of existing and/or resulting interconnecting macropores which might promote resorption and replacement by the surrounding host bone.

As shown in this study, the biodegradability increased with the addition of more β-TCP granules. In vivo biodegradability can be achieved by dissolution or cell-mediated resorption. Micro- or macroporosity of the bone substitute material plays an important role in this biodegradability. The increased porosity of C50 might be responsible for the higher absorption of the implant material. However, biodegrability of a bone substitute depends not only on porosity but also on material properties including Ca/P ratio, crystallinity, and so on[25]. As the reaction of CPC progresses, HA is precipitated[5]. HA is hardly absorbed in vivo, while β-TCP is known to show faster resorption than HA[26]. As revealed by the XRD examination, HA as well as tetracalcium phosphate (TeCP) decreased with an increasing amount of β-TCP. The rate of absorption of C50 might be enhanced by a decreased crystal change from CPC to HA.

Although the increased porosity facilitates biodegrability and bone formation, the result is a reduction in mechanical strength. The results of this study also showed that an increase of β-TCP content resulted in a reduction of compressive strength. Sawamura et al. reported that the compressive strength increased with increasing amounts of HA[13]. The decrease of HA as shown by the XRD examination also was responsible for the lower comprehensive strength. The median compressive strength of C30 was 22 MPa and that of C50 was 13 MPa. The compressive strength of human cortical bone ranges between 90 and 230 MPa, whereas the compressive strength of cancellous bone ranges between 2 and 45 MPa[27][28]. The mechanical strengths of C30 and C50 were almost the same as for cancellous bone. Real et al. succeeded in forming macropores with CPC by adding sodium bicarbonate, but reported that the mechanical strength was only 2.1±0.3 Mpa[29]. Endo et al. formed macropores by mixing collagen I in CPC, but reported that when mixed with 9.1 mass%, the strength decreased to 3.63±0.20 Mpa[30]. Compared to these studies of macropores in CPC, the composite material of CPC paste and porous β-TCP granules had higher and sufficient strength as a bone substitute material applicable to non-load-bearing areas.

Our new material with porous β-TCP granules added to CPC paste had good bioactivity and osteoconductivity. In histological examinations, the newly formed bone was directly in contact with the surface of the implant materials. It was reported that the surface topography is important for cell attachment[31][32]. As shown in the SEM study, the surface roughness of the studied materials was thought to enhance attachment, proliferation and differentiation of anchorage-dependent bone-forming cells[33]. Osteoconductivity is the ability of a material to serve as a scaffold to guide new bone formation. In the results of this study, histological examination revealed bone formation along the surface of the composite of CPC and β-TCP granules. In addition, new bone formation was also observed inside the implant material where bioabsorption occurred. These results suggested that the composite material of CPC paste and porous β-TCP granules had excellent bioactivity and osteoconductivity.

The setting time of CPC paste/β-TCP granules increased with increasing ratio of β-TCP content. However, the setting time of C50 was 18 minutes, which we thought to be within the clinically acceptable range. Setting time correlates with temperature, typically increasing sharply when the temperature is low. In this study, the setting time was measured at body temperature (37℃). However, the setting time would be prolonged if hardening took place under conditions of low temperature[13].

V Conclusion

Based on the results of this study, we believe that the composite created by adding porous β-TCP

granules to CPC paste had good biodegradability and adequate mechanical strength adaptable for bone defects as a bone substitute. If porous β-TCP granules were added as equal wt% of CPC cement (C50), the composite material was almost completely bioabsorbed and replaced by newly formed bone at 36 weeks after implantation. It is thought that C50 is suitable for clinical application and we would like to conduct a clinical study.

Ⅵ Conflict of interest

The authors declare no conflict of interest.

Ⅶ Acknowledgement

We are grateful to Dr. Li Yinghui of Hebei Medical University for providing technical advice. We also would like to thank Dr. Akari Takeuchi of the Department of Chemistry, Faculty of Science, Shinshu University who provided us advice for XRD examination.

References

1) Bohner M, Gbureck U, Barralet JE : Technological issues for the development of more efficient calcium phosphate bone cements : a critical assessment. Biomaterials 26 : 6423–6429, 2005
2) David L, Argenta L, Fisher D : Hydroxyapatite cement in pediatric craniofacial reconstruction. J Craniofac Surg 16 : 129–133, 2005
3) Roozbahani M, Alehosseini M, Kharaziha M, Emadi R : Nano-calcium phosphate bone cement based on Si-stabilized α-tricalcium phosphate with improved mechanical properties. Mater Sci Eng C Mater Biol Appl 81 : 532–541, 2017
4) Sariibrahimoglu K, Wolke JG, Leeuwenburgh SC, Yubao L, Jansen JA : Injectable biphasic calcium phosphate cements as a potential bone substitute. J Biomed Mater Res B Appl Biomater 102 : 415–422, 2014
5) Dorozhkin SV : Bioceramics of calcium orthophosphates. Biomaterials 31 : 1465–1485, 2010
6) Dorozhkin SV : Self-setting calcium orthophosphate formulations. J Funct Biomater 4 : 209–311, 2013
7) Zhang J, Liu W, Schnitzler V, Tancret F, Bouler JM : Calciumphosphate cements for bone substitution : Chemistry, handling and mechanical properties. Acta Biomater 10 : 1035–1049, 2014
8) Yomoda M, Sobajima S, Kasuya A, Neo M : Calcium phosphate cement-gelatin powder composite testing in canine models : Clinical implications for treatment of bone defects. J Biomater Appl 29 : 1385–1393, 2015
9) Kasuya A, Sobajima S, Kinoshita M : In vivo degradation and new bone formation of calcium phosphate cement-gelatin powder composite related to macroporosity after in situ gelatin degradation. J Orthop Res 30 : 1103–1111, 2012
10) Matsumoto G, Sugita Y, Kubo K, Yoshida W, Ikada Y, Sobajima S, Neo M, Maeda H, Kinoshita Y : Gelatin powders accelerate the resorption of calcium phosphate cement and improve healing in the alveolar ridge. J Biomater Appl 28 : 1316–1324, 2014
11) Yaszemski MJ, Payne RG, Hayes WC, Langer R, Mikos AG : Evolution of bone transplantation : molecular, cellular and tissue strategies to engineer human bone. Biomaterials 17 : 175–185, 1996
12) Hollinger JO, Brekke J, Gruskin E, Lee D : Role of bone substitutes. Clin Orthop Relat Res 324 : 55–65, 1996
13) Sawamura T, Mizutani Y, Okuyama M. Obata A, Kasuga T : Compressive strength of calcium phosphate cements prepared using different initial setting temperatures. J Ceram Soc Japan 123 : 59–61, 2015
14) Cao H, Kuboyama N : A biodegradable porous composite scaffold of PGA/beta-TCP for bone tissue engineering. Bone 46 : 386–395, 2010
15) Gao P, Zhang H, Liu Y, Fan B, Li X, Xiao X, Lan P, Li M, Geng L, Liu D, Yuan Y, Lian Q, Lu J, Guo Z, Wang Z : Beta-tricalcium phosphate granules improve osteogenesis in vitro and establish innovative osteo-regenerators for bone tissue engineering in vivo. Sci Rep 6 : 23367, 2016
16) Spector M : Anorganic bovine bone and ceramic analogs of bone mineral as implants to facilitate bone regeneration.

Clin Plast Surg 21 : 437–444, 1994
17) Rawlings CE 3rd : Modern bone substitutes with emphasis on calcium phosphate ceramics and osteoinductors. Neurosurgery 33 : 935–938, 1993
18) Schmitz JP, Hollinger JO, Milam SB : Reconstruction of bone using calcium phosphate bone cements : a critical review. J Oral Maxillofac Surg 57 : 1122–1126, 1999
19) Hayashi M, Takahashi T, Kawaguchi K, Watanabe T, Zhao J, Abiko Y : Connexin 43 expression at an early stage in dog mandibles by β–TCP. Dent Mater J 30 : 58–65, 2011
20) Matsuno T, Nakamura T, Kuremoto K, Notazawa S, Nakahara T, Hashimoto Y, Satoh T, Shimizu Y : Development of beta–tricalcium phosphate/collagen sponge composite for bone regeneration. Dent Mater J 25 : 138–144, 2006
21) Almirall A, Larrecq G, Delgado JA, Martínez S, Planell JA, Ginebra MP : Fabrication of low temperature macroporous hydroxyapatite scaffolds by foaming and hydrolysis of an alpha–TCP paste. Biomaterials 25 : 3671–3680, 2004
22) Link DP, van den Dolder J, van den Beucken JJ, Habraken W, Soede A, Boerman OC, Mikos AG, Jansen JA : Evaluation of an orthotopically implanted calcium phosphate cement containing gelatin microparticles. J Biomed Mater Res A 90 : 372–379, 2009
23) Matsumoto G, Sugita Y, Kubo K, Yoshida W, Ikada Y, Sobajima S, Neo M, Maeda H, Kinoshita Y : Gelatin powders accelerate the resorption of calcium phosphate cement and improve healing in the alveolar ridge. J Biomater 28 : 1316–1324, 2014
24) Karageorgiou V, Kaplan D : Porosity of 3D biomaterial scaffolds and osteogenesis. Biomaterials 26 : 5474–5491, 2005
25) LeGeros RZ : Properties of osteoconductive biomaterials : calcium phosphates. Clin Orthop Relat Res 395 : 81–98, 2002
26) Hing KA : Bone repair in the twenty–first century : biology, chemistry or engineering? Philos Trans A Math Phys Eng Sci 362 : 2821–2850, 2004
27) An YH : Mechanical properties of bone. In : Mechanical testing of bone and the bone–implant interface, pp 41–64, Boca Raton, Florida, 2000
28) Ginebra MP : Calcium phosphate bone cements. In : Orthopaedic bone cements. 1st ed, pp 206–230, Woodhead Publishing Limited, Cambridge, 2008
29) del Real RP, Wolke JG, Vallet–Regí M, Jansen JA : A new method to produce macropores in calcium phosphate cements. Biomaterials 23 : 3673–3680, 2002
30) Endo H, ltatani K, Umeda T, Koda S : Properties of calcium phosphate paste with blood containing collagen. Effect of collagen form in the kneading operation. J Soc Inorg Mater Japan 13 : 105–111, 2006
31) Ciapetti G, Ambrosio L, Savarino L, Granchi D, Cenni E, Baldini N, Pagani S, Guizzardi S, Causa F, Giunti A : Osteoblast growth and function in porous poly–caprolactone matrices for bone repair : a preliminary study. Biomaterials 24 : 3815–3824, 2003
32) Jingwei Z, Melis T, Xiaoman L, Erik V, Davide B, Lorenzo M, Joost D, Clemens A, Paul C, Martin M, Huipin Y : Topography of calcium phosphate ceramics regulates primary cilia length and TGF receptor recruitment associated with osteogenesis. Acta Biomater 57 : 487–497, 2017
33) Yuan H, Kurashina K, Bruijn JD, Li Y, Groot K, Zhang X : A preliminary study on osteoinduction of two kinds of calcium phosphate ceramics. Biomaterials 20 : 1799–1806, 1999

(2017. 11. 22 received ; 2017. 12. 28 accepted)